Lavajatus moroi, new cavernicolous Subulininae from Ceará, Brazil

(Gastropoda, Eupulmonata, Achatinidae)

Luiz Ricardo L. Simone

Lavajatus moroi is a new genus and species found in cave environment from Santa Quitéria region, Ceará, Brazil. It is mainly characterized by the very elongated shell measuring about 30 mm, the growth is uniform, adult shell of ~28 whorls, and the shell profile is rather straight. The species has an extraordinary capacity of retraction inside the shell, keeping empty from $\frac{1}{3}$ to $\frac{1}{2}$ of the shell length when retracted. Anatomically, lung lacking developed vessels; ureter entirely tubular; kidney wide, with narrow anterior projection; genital structures mostly located inside anterior half of the haemocoel; lack of jaw, esophagus very narrow; large pair of retractor muscles of buccal mass (*m2*), with a branch passing through the nerve ring; odontophore lacking horizontal muscle (*m6*), with cartilages ~$\frac{3}{5}$ fused with each other; spermoviduct having two regions, being the anterior one normally bearing young specimens; and nerve ring having a large visceral/subesophageal ganglion. The dissection of the intrauterine young specimens, which normally have a swollen head and a posterior pedal flap, revels some interesting ontogenetic features, such as the extreme elongation of some structures, e. g., the lung and digestive tubes, the repositioning of some haemocoel structures, and the modification of the nerve ring (appearance of the pleural ganglia, fusion and migration towards anterior of the subesophageal ganglia) during the development. Comparison with known subulinines is performed, including accounts on the youth intrauterine development. The new species is almost troglobian, except for the presence of eyes. Paper register: urn:lsid:zoobank.org:pub:14A47DB2-EA91-45F4-8164-B731E2C1C67D

Luiz Ricardo L. Simone, Museu de Zoologia da Universidade de São Paulo, Cx Postal 42391, 04218-970 São Paulo, SP, Brazil;
e-mail: lrsimone@usp.br, lrlsimone@gmail.com; OrcID: 0000-0002-1397-9823

Introduction

Description of new taxa in land malacofauna from Brazil is a routine, even including new genera, mainly in cave environment (e. g., Simone 2012a,b, 2013). This shows how weak is the knowledge on the invertebrate fauna in such megadiverse region.

This paper refers to another discover, samples of a considerably large gastropod found in caves from Santa Quitéria, Ceará, Brazil, in such conchological and anatomical analysis showed a new entity in specific and generic levels, belonged to the achatinoidean subfamily Subulininae (Achatinidae). The morphological characters suggest troglobian adaptations (except for the presence of eyes), and some anatomical idiosyncrasies that change some concepts on the pulmonate anatomy.

The subulinines are mostly small-sized snails, leaving on soil and leaves litter, despite some few species being large (e. g., *Neobeliscus calcareus* (Born, 1780), over 10 cm – Simone 2006) and some even carnivore (e. g., *Paropeas* Pilsbry, 1906 – Naggs 1994).

Their shells normally are elongated-turriform and fragile, however, one of more remarkable features is the ovoviviparity, in such some eggs, embryos and even young specimens are found inside uterus (Mead 1950, Budha et al. 2017). They occur worldwide, mostly in tropical regions, in a bulk of more than 1300 species (Pilsbry 1906, Naggs 1994), with some species having medical and veterinary importance (e. g., Dutra 1988, Almeida & Bessa 2001).

In contrast to the high diversity of the subulinines is the scanty knowledge on their taxonomy and anatomy (Naggs 1994). Their relative uniform and simple shells are practically the single structure used for taxonomy, with some influence of the genitalia and radula characters, which has been replaced by molecular approaches (e. g., Fontanilla et al. 2017). Phenotypical approaches are scanty, the present paper has the intention to contribute in this area. Additionally, seizing the opportunity of the presence of young specimens nesting in the uterus, their comparative dissection can also reveal interesting data on the ontogeny and development, which are also investigated herein.

Material and methods

The specimens were donated fixed in 70 % ethanol. The specimens' extraction was by cautious shell cracking. The dissections were performed in a stereomicroscope, with the specimens immersed in ethanol. The dissections techniques are as in Simone (2011). All anatomical drawings were performed with the aid of a camera lucida, each final drawing is a compilation of several specimens. Digital photos were also obtained in all dissection steps, some of them shown here. Radulae were examined in scanning electron microscope (SEM) in the MZSP Laboratory of Electron Microscopy. Odontophore terminology follows mainly Simone (2011).

Anatomical abbreviations: *ad*, albumen gland duct; *ag*, albumen gland; *an*, anus; *ar*, adrectal sinus; *au*, auricle; *bc*, bursa copulatrix; *bd*, bursa copulatrix duct; *bg*, buccal ganglion; *bm*, buccal mass; *bv*, blood vessel; *cc*, cerebral commissure; *ce*, cerebral ganglion; *cm*, columellar muscle; *cn*, cerebro-pedal and cerebro-pleural connectives; *co*, collar vessel; *cv*, pulmonary (efferent) vein; *da*, digestive gland anterior lobe; *dc*, dorsal chamber between dorsal folds of oral cavity; *dd*, duct to digestive gland; *df*, dorsal fold of buccal mass; *dg*, digestive gland posterior lobe; *ef*, esophageal folds; *eo*, spermoviduct; *ep*, epiphallus; *es*, esophagus; *ff*, foot posterior flap (pedal vesicle); *fo*, free oviduct; *fp*, genital pore; *ft*, foot; *gf*, genital fold; *gg*, genital gland; *gl*, optical ganglion; *go*, gonad; *gp*, pleural ganglion; *gs*, germ

of genital system; *hd*, hermaphrodite duct; *he*, head; *in*, intestine; *ki*, kidney; *m1–m10*, extrinsic and intrinsic odontophore muscles; *mb*, mantle border; *mf*, mantle fold; *mg*, mantle gland; *mj*, jaw and peribuccal muscles; *mo*, mouth; *nc*, nuchal connection between head and mantle border; *ne*, nephrostome; *nv*, nerve; *oc*, odontophore cartilage; *od*, odontophore; *om*, ommatophore; *ov*, egg in uterus; *pc*, pericardium; *pe*, penis; *pg*, pedal gland; *pm*, penis muscle; *pn*, pneumostome; *pp*, pedal ganglion; *pt*, prostate; *pu*, pulmonary cavity; *pv*, pneumostome right flap; *ra*, radula; *rn*, radular nucleus; *rs*, radular sac; *rt*, rectum; *sa*, salivary gland aperture; *sd*, salivary gland duct; *sg*, salivary gland; *sl*, sublingual fold; *sr*, seminal receptacle; *st*, stomach; *sy*, statocyst; *te*, tentacle; *ua*, ureter aperture; *up*, primary ureter; *ur*, secondary ureter; *ut*, uterus; *vd*, vas deferens; *ve*, ventricle; *vg*, vagina; *vi*, visceral ganglion.

Institutional abbreviation: MZSP = Museu de Zoologia da Universidade de São Paulo, Brazil.

Taxonomy

Lavajatus gen. nov.

urn:lsid:zoobank.org:act:8313B992-480D-496D-831D-302E9B22F71A

Diagnosis. Shell of relative large size (adult ~30 mm), multispiral (adult mean ~27 whorls), turriform, whorls profile relatively straight (suture weakly deep); wall thin, translucent. Indeterminate growth, peristome simple, not deflected, slightly squared. Protoconch rounded, ~5 first teleoconch whorls with width increment larger than remaining teleoconch whorls (with weak successive with increment). Pulmonary venation reduced. Urinary aperture and anus opening directly outside. Seminal receptacle as series of small chambers; albumen chamber absent. Penis with epiphallus of thick muscular chamber. Viviparity. Nerve ring with large subesophageal/intestinal ganglion located close to it.

Type species. *Lavajatus moroi* spec. nov.

List of included taxa. *L. moroi*.

Etymology. The generic name is a Latinization of the Portuguese words Lava Jato (car wash), an allusion to the Lava-Jato Operation, which designates a conjunct of investigations of Federal Police of Brazil, mostly investigating corruption crimes. The translucency of the shell, revealing the occult inner structures, is an afflatus.

Discussion. See below.
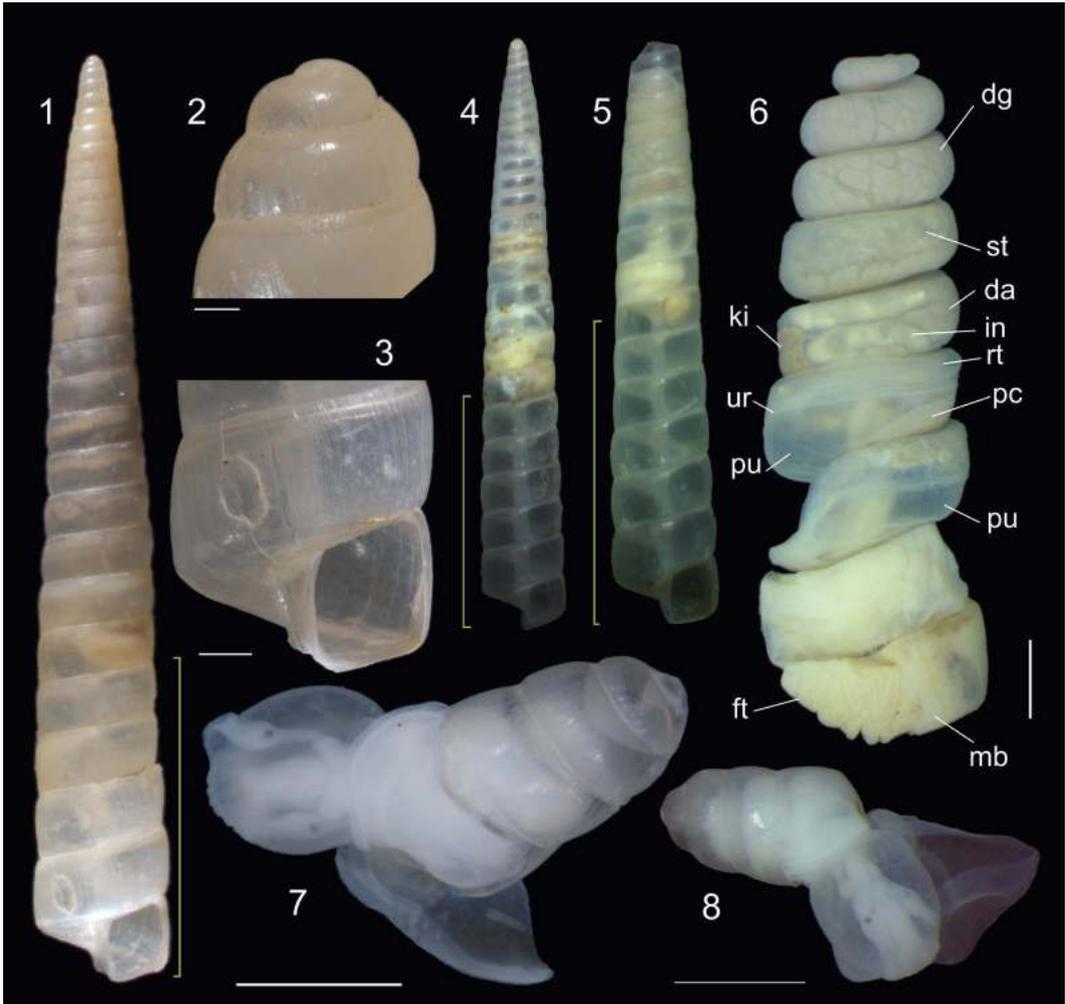
Figs 1–8. *Lavajatus moroi*. **1.** Holotype MZSP 131060, apertural view (L 34.7 mm); **2.** same, detail of protoconch, scale = 0.5 mm; **3.** same, detail of aperture, frontal view, scale = 1 mm; **4.** paratype MZSP 131066#1, apertural view (L 30.8 mm); **5.** paratype MZSP 131066#2, apertural view (L 23.0 mm); **6.** same, specimen extracted from shell, scale = 1 mm. **7–8.** young specimen extracted from uterus, dorsal view, scales 1 mm. Yellow marks showing degree of shrinkage of specimens.

Lavajatus moroi spec. nov.
Figs 1–41

urn:lsid:zoobank.org:act:54DF2775-A07F-4333-8E81-09178F033A5C

Types. Holotype: MZSP 131060. Paratypes: BRAZIL. Ceará; Santa Quitéria, Caves (26–28.iii.2013), MZSP 131061, 4°33'47.556"S 39°46'44.815"W, 2 spm (Sta. QUI02), MZSP 131062, 4°33'49.509"S 39°46'45.434"W, 2 spm (Sta. QUI06), MZSP 131063, 4°33'47.522"S 39°46'46.048"W, 1 spm (Sta. QUI07), MZSP 131064, 4°33'47.392"S 39°46'45.658"W, 1 spm (Sta. QUI08), MZSP 131065, 4°33'50.651"S 39°46'44.169"W, 1 spm (Sta. QUI-01), MZSP 131066, 4°33'47.328"S 39°46'45.204"W, 1 spm (Sta. QUI10), MZSP 131067, 4°33'50.651"S 39°46'44.169"W, 2 spm (Sta. QUI01).

Type locality. BRAZIL. Ceará; Santa Quitéria, Cave, 4°33'50.651"S 39°46'44.169"W [Sta. QUI01; Sizauskas & Felice col, 26–28.iii.2013]

Description

Shell (Figs 1–5). Adult shell around 30 mm, turriform, very elongated, multispiral; apex pointed;

175

greatest width on last whorl; width ~15 % shell length. First 5–7 whorls widening considerably, initial spire angle ~20°; after this stretch, teleoconch gradually widening weakly, projecting spire angle ~10° (Figs 1, 4). About 50 % specimens with autotomy of more apical whorls (Fig. 5), with hole blocked by rustic calcified cover. Basal colour uniform pale beige, walls relatively thin, fragile, translucent (Figs 4, 5) to semi-translucent (Figs 1–3). Protoconch of 2 whorls, relatively rounded, with small initial projected area (Figs 2, 7, 8), ~2.5 % of length; absolutely smooth, glossy; transition to teleoconch unclear, marked by gradual appearance of weak axial undulations. Teleoconch smooth, except for relatively uniform, narrow axial undulations (Fig. 3), ~50 in penultimate whorl. Whorls profile weakly convex, almost straight. Suture weakly deep, marked, slightly oblique ~95° in relation to columellar axis. Aperture orthocline (Fig. 3), squared; ~9 % of shell length, ~35 % of shell width. Peristome not reflected, undetermined growth. Body whorl ~18 % of shell length. Umbilicus narrow. Columella as narrow, hollow tube, weakly zigzagging along shell axis (Figs 4–5).

Head-foot (Figs 6, 21, 24). Of normal shape. Colour uniformly clear. Columellar muscle initially thick, gradually becoming thinner along ~5 whorls; posterior end bluntly pointed. Haemocoel narrowing considerably after 2 whorls, becoming ~$\frac{1}{3}$ of columellar muscle width. High capacity of shrinkage inside shell, distancing from $\frac{1}{3}$ (Figs 1, 4) to $\frac{1}{2}$ (Fig. 5) of shell length from aperture (Figs 1, 4, 5: yellow bars).

Mantle organs (Figs 6, 21–23, 29). Mantle border (mb) thick, lacking pigments, except for pale brown mantle glands (Fig. 23: mg) seen by translucency. Pneumostome (pn) protected by ventral, right simple flap (pv), with ~$\frac{1}{4}$ of aperture length. Dorsal fold not developed, immersed in mantle border (Fig. 22: mb). Pneumostome (pn) ~$\frac{1}{5}$ of aperture length, bearing beyond air entrance, ureter aperture (Fig. 23: ua) and anus (an), both turned directly outside; aperture of ureter ample, oblique. Anus as separated aperture located at right from pneumostome (Fig. 23: an) by side of urinary aperture. Lung of ~4 whorls in length, narrow, elongated. Pulmonary vessels inconspicuous, seen in higher magnifications even in region just posterior to mantle border (Fig. 23), only collar vessel slightly more developed (Fig. 23: co), remaining regions almost smooth. Pulmonary vein (cv) running longitudinally between middle and right thirds of pallial cavity roof, gradually approaching from median line and becoming visible in posterior end (Fig. 29: cv). Reno-pericardial area reddish-beige, slightly rectangular, located posteriorly at middle level of posterior end, occupying ~$\frac{1}{6}$ of cavity length

and ~80 % of its width (details below). Rectum (rt) and ureter (ur) narrow, running along right edge.

Visceral mass (Figs 6, 21). ~6–10 whorls in length. Both digestive gland lobes pale greenish beige in colour (dg). Anterior lobe (Fig. 24: da) flattened, occupying ~$\frac{1}{3}$ width of visceral two first whorls, located just posteriorly to pallial cavity, continuous to kidney, creased by intestinal loops. Posterior lobe (dg) with 5–9 spiral whorls, with ~70 % of visceral volume. Stomach (st) of 2-whorls, ~$\frac{1}{10}$ of visceral volume, located between both digestive gland lobes, about one whorl posterior to pallial cavity (Fig. 24: st). Digestive tubes (described below) surrounding anterior end of digestive gland posterior lobe. Gonad small, multi-lobed, cream colour, encased between posterior lobe of digestive gland and columella 3–4 whorls posterior from stomach, occupying ~$\frac{1}{30}$ of visceral volume (Fig. 33: go).

Circulatory and excretory systems (Figs 21, 29). Pericardium (pc) ~4 times as long as wide, located at posterior whorl of pallial roof; occupying ~5 % of lung area. Auricle (au) located anteriorly, as continuation from pulmonary vein (cv), slightly smaller than ventricle (ve). Kidney (ki) simple, entirely solid, dorso-ventrally flattened; size ~70 % of reno-pericardial area; somewhat rectangular, width ~$\frac{1}{2}$ of length; small anterior projection compressed between primary ureter and pericardium, prolonging it more $\frac{1}{2}$ kidney length towards anterior. Nephropore small, longitudinal slit in anterior-left corner of primary ureter (up), turned right (Fig. 29: ne – by transparency). Primary and secondary ureter complete and closed (tubular); primary ureter (up) lying on right edge of kidney anterior narrow projection towards posterior and right, after forming strong curve, running afterwards anteriorly, as secondary ureter (ur) along entire left edge of rectum. Adrectal sinus well-developed along entire rectum length (Fig. 29: ar).

Digestive system (Figs 24–32). Oral tube wide, thick muscular (Fig. 30: mj). Jaw wanting, in its place wide transverse groove (Fig. 30: above df). Buccal mass spherical, with ~$\frac{1}{7}$ of haemocoel volume (Figs 24, 28: bm). Dorsal surface of oral cavity with well-developed pair of dorsal folds (Fig. 30: df), width of each ~$\frac{1}{3}$ of dorsal wall width; separated from each other by dorsal chamber (dc) as wide as each fold. Sublingual fold relatively large, located ventral to odontophore up to region close to mouth (Fig. 30: sl). Odontophore rounded, ~60 % of buccal mass volume (Figs 26, 28, 30: od). Odontophore muscles (Figs 26–28, 30–32): **mj**, peribuccal muscles originating in outer-ventral surface of odontophore cartilages (Fig. 32: mj), running towards dorsal, splaying in dorsal wall
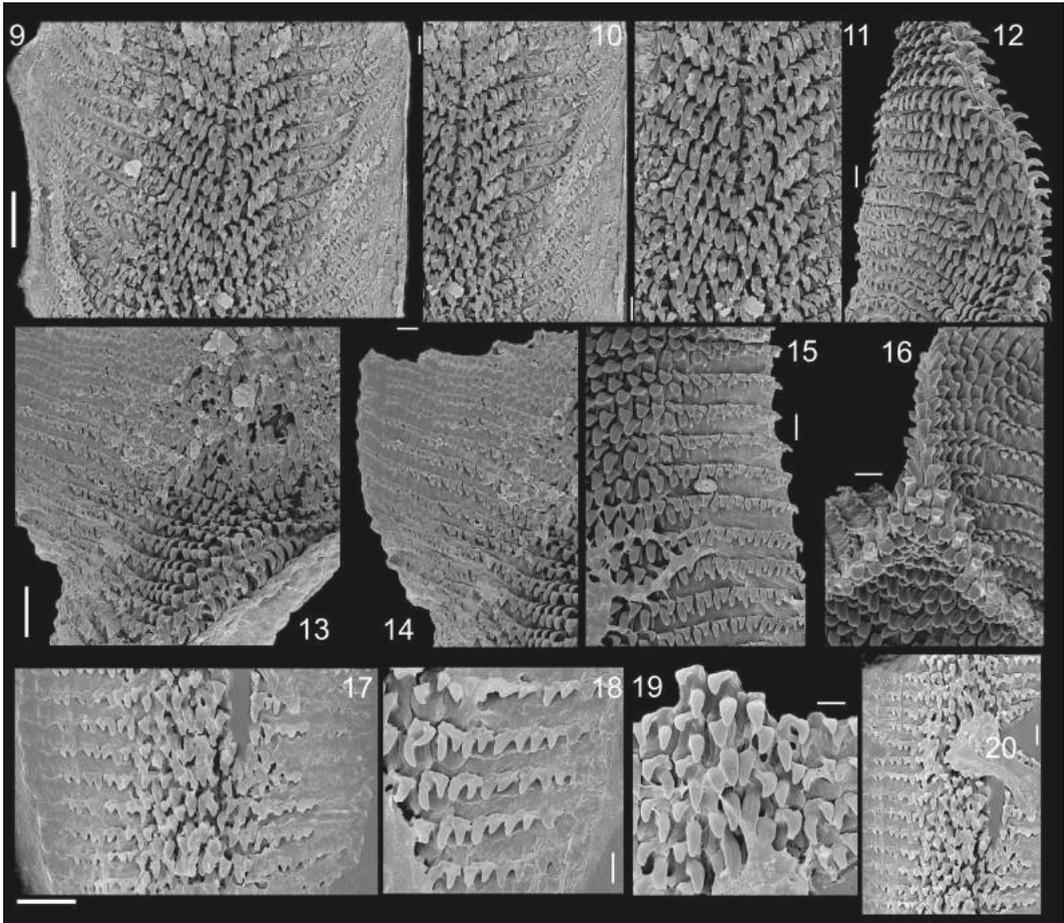
Figs 9–20. *Lavajatus moroi*, radulae in SEM. **9–16.** Adult specimens. **9.** Wide view, scale = 50 µm; **10.** same, detail of right half, scale = 20 µm; **11.** same, detail of central region, scale = 20 µm; **12.** another specimen, bended radula ribbon, scale = 20 µm; **13.** another specimen, wide view, scale = 50 µm; **14.** same, detail of left region, scale = 20 µm; **15.** same, detail of right region, scale = 20 µm; **16.** same, bended region, scale = 20 µm. **17–20.** Intrauterine young specimen. **17.** Wide view, scale = 20 µm; **18.** same, detail of right half, scale = 5 µm; **19.** another specimen, detail of central region, scale = 5 µm; **20.** same, detail of left half, scale = 5 µm.

of oral tube (Fig. 31: *mj*); *m1*, jugal muscles covering entirely haemocoelic structures, more concentrated close to mouth; *m1l*, small pair of lateral protractors jugal muscles, originating in lateral surface of haemocoel close to mouth, running towards posterior, inserting in lateral region of haemocoel wall in posterior level of odontophore (Figs 26–28: *m1l*); *m2*, strong pair of retractor muscles of buccal mass, or radular muscles, originating as single thick bundle in columellar muscle, being mostly as thick and wide as columellar muscle (Fig. 28: *m2*), running anteriorly close to median line along almost entire haemocoel length, inserting as two different bundles: medial, smaller bundle inserting in ventro-posterior edge

of odontophore cartilages (Figs 31, 32: *m2c*), lateral, larger bundle running further anteriorly, inserting in ventral region of mouth (Figs 26–28: *m2*); *m4*, main pair of dorsal tensor muscles of radula, very thick, originating in postero-medial region of odontophore cartilages (Figs 31–32: *m4*), surrounding outside and medially cartilages, inserting in subradular membrane in its region correspondent to buccal cavity; *m5*, pair of thick auxiliary dorsal tensor muscles of radula, originating in postero-ventral region of odontophore cartilages (Figs 31–32: *m5*), along ~half of their length, running towards median line flanking *m4* postero-medial edge, inserting in subradular membrane ventral of *m4* insertion; *m6*, horizontal

177
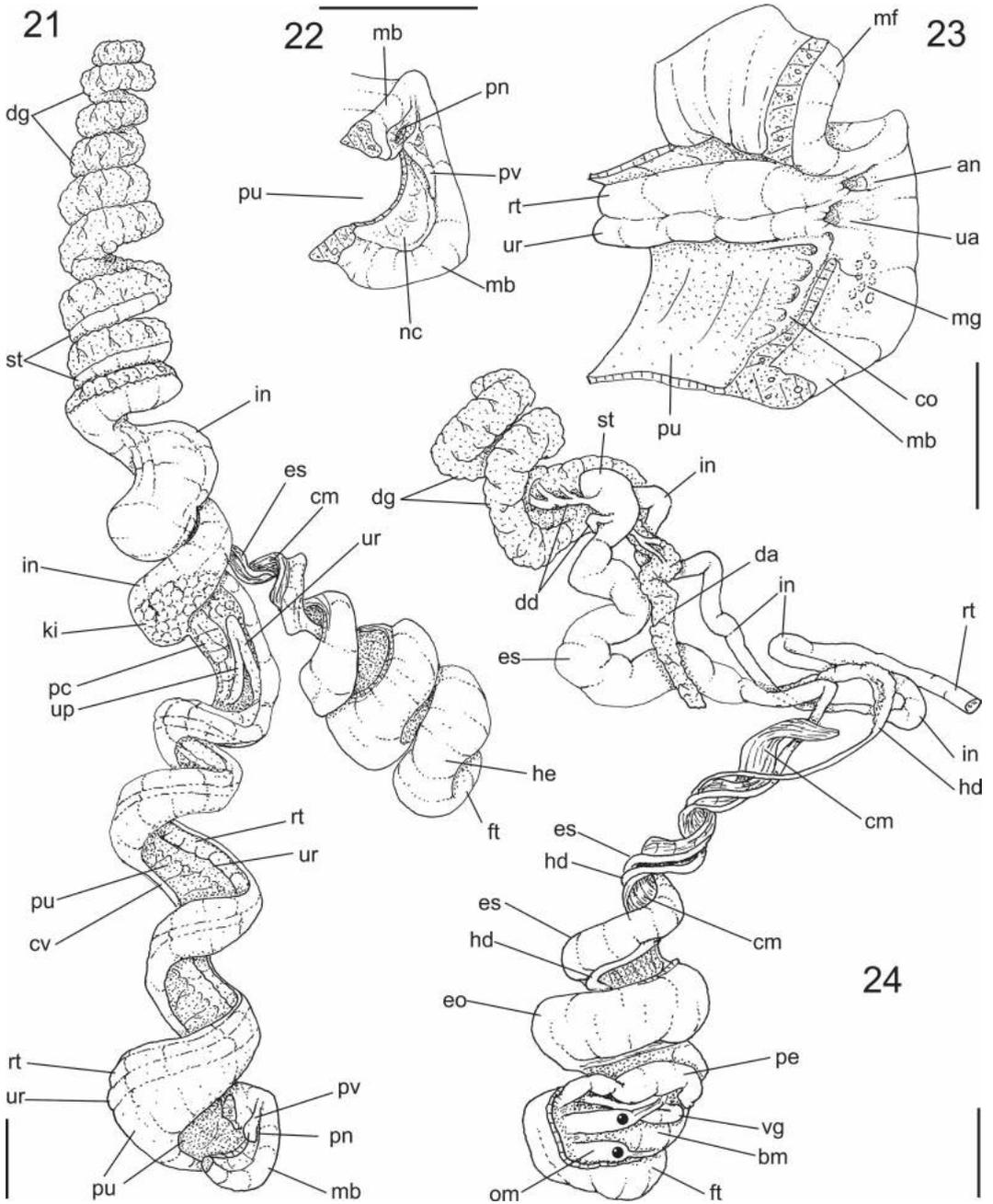
Figs 21–24. *Lavajatus moroi* anatomy. **21.** Whole specimen removed from shell, pallial cavity (left) partially separated from head-foot (right) by longitudinal sections; **22.** mantle border, frontal view, head-foot removed; **23.** region of pneumostome, ventral view, inner flap of pneumostome (*mf*) sectioned and deflected upwards, pallial gland (*mg*) seen by translucency; **24.** same as Fig. 21 with diaphragm and pallial floor entirely removed, pallial cavity and reno-pericardial structures removed, first visceral whorls partially uncoiled, structures deflected. Scales = 2 mm.
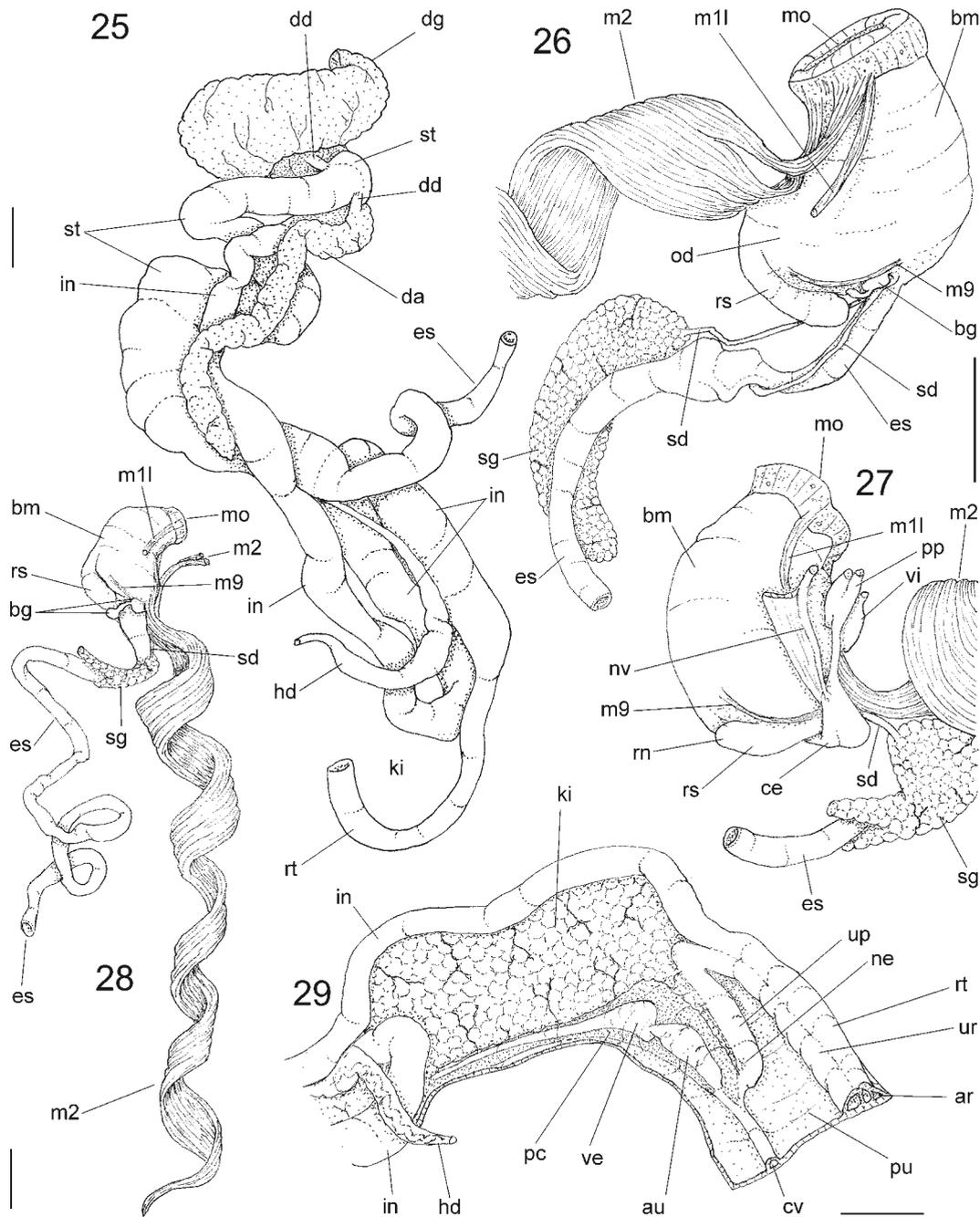
Figs 25–29. *Lavajatus moroi* anatomy. **25.** Dissected first whorls of visceral mass, most structures partially deflected, mostly ventral view; **26.** foregut, left view; **27.** same, right view, nerve ring still in situ; **28.** foregut, whole view, nerve ring removed; **29.** last whorl of visceral mass, ventral view, mostly showing reno-pericardial structures, and posterior end of pallial cavity. Scales = 1 mm.
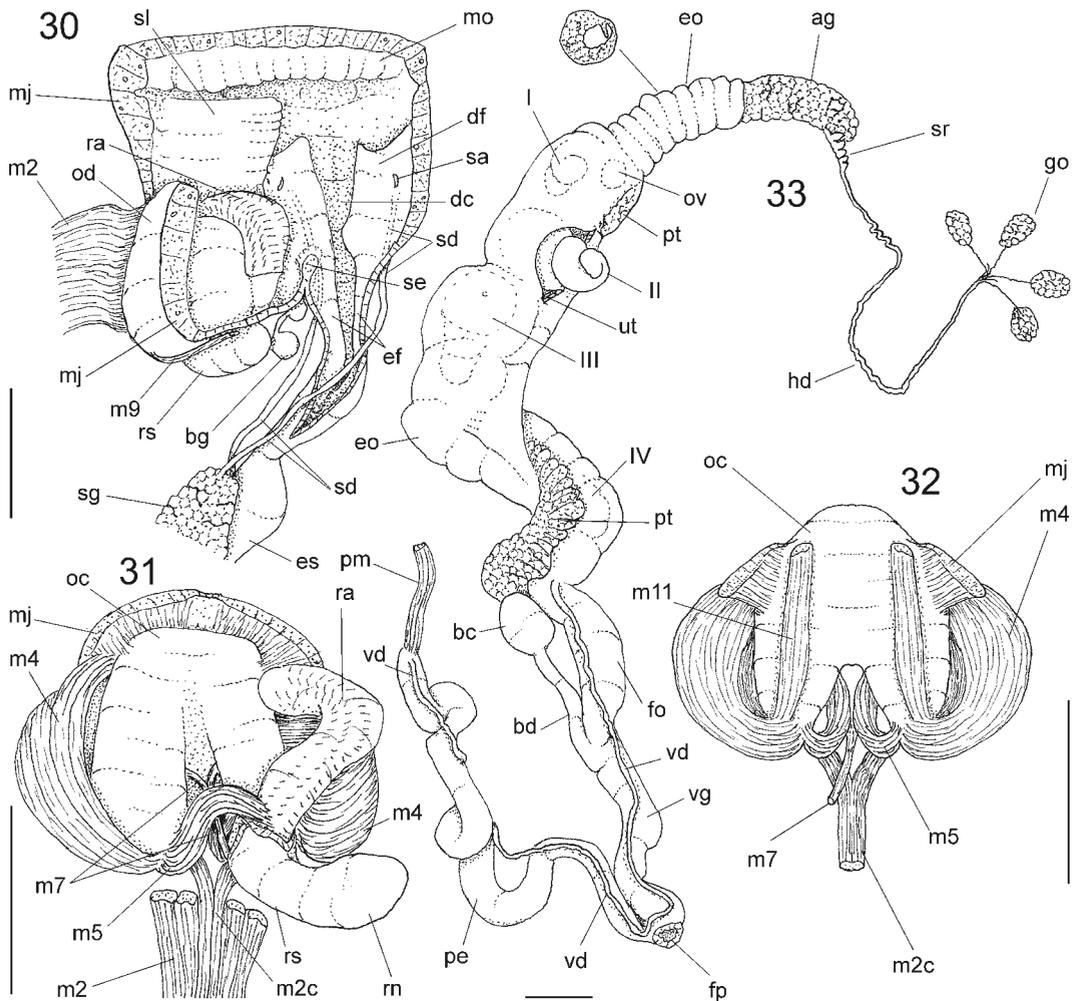
Figs 30–33. *Lavajatus moroi* anatomy. **30.** Foregut, mostly ventral view, mostly opened longitudinally with odontophore (*od*) deflected to left; **31.** odontophore, dorsal view, most muscles deflected, radula removed and deflected to right with *m5* pair still attached; **32.** odontophore, ventral view, superficial layer of muscles and structures removed. **33.** genital system, whole ventral view, transverse section in indicated region of spermoviduct shown, young specimens inside uterus indicated by Roman numerals, being one of them (II) artificially displaced by small longitudinal section. Scales = 1 mm.

muscle absent; *m7*, small pair of muscles originating in middle-posterior level of cartilages central edge, in posterior level of cartilages fusion (Fig. 31: *m7*), running medial-posteriorly inside radular sac, inserting splaying in dorso-postero inner surface of radular sac (Figs 31–32: *m7*); *m9*, pair of small, narrow, superficial and thin muscles flanking both sides of radular sac, oriented dorso-ventrally (Figs 26–28, 30: *m9*); *m11*, pair of narrow ventral tensor muscles of radula, originating in ventro-lateral surface of posterior region of cartilages, running close to car-

tilages towards anterior, inserting in ventral end of subradular membrane (Fig. 32: *m11*). Odontophore non-muscular structures (Figs 31–32): *oc*, odontophore cartilages flattened, elliptical, anterior region slightly projected anteriorly close to median line, ~twice longer than wide, fused with each other along ~³/₅ in their anterior-medial edge (Figs 31–32: *oc*), anterior end roughly rounded; *sc*, subradular cartilage, with expanding region in buccal cavity protecting subradular membrane. Radular sac short, extending beyond odontophore ~ half odontophore
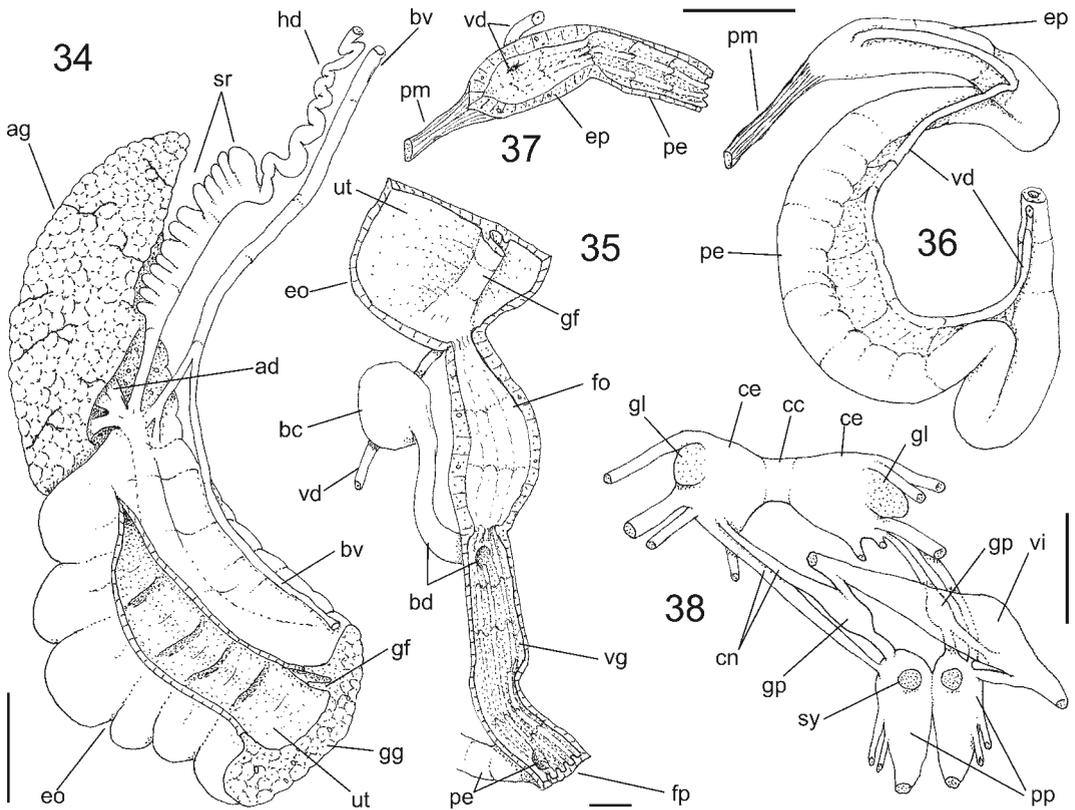
Figs 34–38. *Lavajatus moroi* anatomy. **34.** Genital system, middle region, ventral view, base of albumen gland (*ag*) partially removed to show its duct, spermoviduct (*eo*) opened longitudinally; **35.** genital system, anterior region entirely opened longitudinally, showing inner surfaces; **36.** penis, ventral view; **37.** penis, detail of posterior region opened longitudinally; **38.** central nervous system (nerve ring), ventral view, visceral ganglion (*vi*) seen as transparent to show structures dorsal to it. Scales = 0.5 mm.

length (Figs 26–28, 31: *rs*). Radular nucleus slightly expanded (Fig. 31: *rn*). **Radula** (Figs 9–16) slightly longer than odontophore, adult with ~70 rows. Radula rows in wide chevrons (Figs 9, 11, 14), teeth similar-shaped with each other; more central teeth with ~4 % of radula width (Fig. 10); 20–24 pairs of teeth per row. Division between lateral and marginal teeth somewhat clear, marked by abrupt decrease of teeth size. **Rachidian** tooth wanting. **Lateral teeth** 8–10 pairs gradually smaller towards lateral; each tooth with rectangular base, antero-posteriorly elongated, ~1.5 times longer than wide; pair of tall, arched cusps, external cusp slightly more anterior than medial cusp; cusps positioned alternately with neighboring teeth (Figs 11, 12, 15, 16); each cusp tongue-like, arched, ~1.5 times longer than base if straightened; cusps tip sometimes pointed, mostly rounded (Fig. 11). **Marginal teeth** similar to lateral teeth, except for being shorter, ~1/3 of lateral teeth

length, but with about same width; pair of cusps of each tooth also intercalated (Figs 9, 10, 13, 15); distance between rows in marginal teeth ~twice times longer than teeth length (Figs 14, 15). Salivary glands covering esophagus in its region preceding its anterior 1/8 (Fig. 28: *sg*), forming two elongated, white, thick masses, ~80 % fused with each other. Each salivary duct differentiable in anterior side of glands, very narrow, slightly iridescent (Figs 26, 27: *sd*). Salivary duct running in both sides of esophageal origin, penetrating buccal mass wall in region close to buccal ganglia (Fig. 30: *sd*), running immersed in buccal dorsal wall along ~1/2 its length (Fig. 30: *sd*). Salivary ducts opening in middle level of dorsal folds (Fig. 30: *sa*).

Esophagus 6-whorl long, narrow since its origin (Fig. 28: *es*), narrowing further along its length (Fig. 24: *es*); walls relatively uniform, lacking clear subdivisions (Figs 25, 28: *es*); inner surface simple;

pair of narrow, longitudinal folds, continuation from buccal cavity dorsal folds (Fig. 30: *df*), running all along esophagus, located close from each other. Esophageal insertion in stomach unclear, marked by gradually enlargement of posterior esophagus (Fig. 24: "*es*" at top). Stomach plus posterior enlarged esophagus (Figs 6, 21, 25: *st*) relatively narrow, ~3-whorl long, occupying ~half local visceral whorls; position described above (visceral mass). Gastric walls thin, flaccid, translucid (Fig. 6: *st*); inner surface smooth. Intestinal origin on left side, both close to columella. Ducts to digestive gland located relatively close from each other, in posterior-most gastric curve (Figs 24, 25: *dd*). Duct to anterior lobe of digestive gland abruptly curving dorsally and anteriorly (Fig. 34: *dd*-inferior). Duct to posterior lobe of digestive gland located short distance posterior from anterior duct, directed towards posterior (Fig. 24: *dd*-superior). Intestine initially as wide as stomach, gradually narrowing up to ~half this width along its wide, sigmoid, ~2-whorl loop in anterior lobe of digestive gland, pressed by narrow space, plus kidney and anterior lobe of digestive gland (Figs 6, 21, 24, 25: *in*). Rectum and anus position described above (pallial cavity) (Figs 21, 23: *rt*, *an*). Anus sessile, slightly oblique, directly turned outside; inner surface smooth (Fig. 23: *an*).

Genital system (Figs 33–37). Gonad position described above (visceral mass), composed of 4–5 relatively small lobes with minute digitiform acini (Fig. 33: *go*) immersed in digestive gland. Hermaphroditic duct (Figs 33, 34: *hd*) 4-whorl long, very narrow, running along 2 posterior whorls of haemocoel (Fig 24: *hd*); mostly weakly coiled, except for more coils in middle third, region covered by transparent membrane (Fig. 24: *hd*-superior); before and afterwards becoming narrow, almost not-coiled (Fig. 33: *hd*). Seminal receptacle (Figs 33, 34: *sr*) as series of 12–14 somewhat irregular-sized, small chambers restricted to right side, successively decreasing towards anterior; size ~2–3 times hermaphroditic duct width. Fertilization complex simple, located at narrow and elongated base of seminal receptacle (Fig. 34) as duct of seminal receptacle and continuation from hermaphroditic duct; ~half length of receptacle. Fertilization complex totally immersed in albumen gland (Fig. 34, with anterior part of gland removed), inserting in posterior end of spermoviduct, in base albumen gland ducts (Fig. 34: *ad*). Albumen gland (Figs 33, 34: *ag*) relatively small (~$\frac{1}{15}$ genital length, ~$\frac{1}{3}$ whorl) solid, white, elliptical. Albumen gland ducts subterminal, divided in 3, connected to distal end of spermoviduct (Fig. 34: *ad*). Albumen chamber wanting. Spermoviduct restricted to anterior half of haemocoel (Fig. 24: *eo*), 3–4 whorl long, ~$\frac{1}{3}$ of speci-

mens with it simple, empty; remaining specimens possessing two regions: posterior region, ~$\frac{1}{5}$ its length, ~$\frac{1}{2}$ narrow, walls thick glandular, successively folded transversally (Fig. 33: *eo*-superior, see transversal section shown there, Fig. 34: *gg*); anterior region, ~$\frac{4}{5}$ long, thinner walls, nesting internally 4–6 young forms as follows: posterior-most simple egg, 0.4 mm long, with non-calcified husk (Fig. 33: *ov*), followed by young specimen only with protoconch shell (2 whorls), ~1 mm long (Fig. 33: I), followed by 3–5 same-sized young specimens, with 4-whorl shell (2 of protoconch, 2 of teleoconch) (Figs 7, 8), ~2 mm long (Fig. 33: II, III, IV) (more details on young, intrauterine specimens below – ontogeny). Prostate gland occupying ~$\frac{1}{3}$ of spermoviduct surface and ~$\frac{1}{4}$ its volume (Fig. 33: *pt*), more concentrated anteriorly. Uterus occupying ~$\frac{3}{4}$ of spermoviduct space, containing above mentioned young specimens (Figs 33–35: *ut*). Sperm grove simple all along spermoviduct, protected ventrally by tall fold (Figs 34, 35: *gf*). Sperm groove abruptly ending ~1-whorl posterior to genital pore, giving origin to free vas deferens (Fig. 35: *gf*–*vd*). Vas deferens running attached to anterior genital ducts, contouring it close to genital pore (Fig. 33: *vd*), flanking penis, connected to it by transparent membrane (Fig. 36: *vd*). Free oviduct with ~$\frac{1}{6}$ spermoviduct length (Fig. 33: *fo*), thick walls, internally with 3–4 broad, low longitudinal folds (Fig. 34: *fo*). Vagina ~$\frac{1}{6}$ spermoviduct length (Fig. 33: *vg*); inner surface simple, with 4–5 longitudinal, low, narrow folds slightly equidistant from each other (Fig. 35: *vg*). Bursa copulatrix ~$\frac{1}{6}$ of spermoviduct length, located inside haemocoel (instead of close to pericardium as usual); bursa duct ~$\frac{1}{3}$ width as adjacent spermoviduct (Figs 33, 35: *bd*); bursa oval, ~$\frac{1}{3}$ of albumen gland size (Figs 33, 35: *bc*). Penis ~$\frac{1}{2}$ of spermoviduct length, ~$\frac{1}{2}$ its anterior width (Fig. 33: *pe*); penis muscle inserting terminally (Figs 33, 36, 37: *pm*), running posteriorly along mid region of columellar muscle (instead of diaphragm), being ~$\frac{1}{8}$ width of columellar muscle plus *m2* along its length. Epiphallus ~$\frac{1}{6}$ penis' length, located as short terminal continuation of penis (Figs 36, 37: *ep*), walls thick muscular, inner surface tight, almost smooth, except for narrow, longitudinal grooves (Fig. 37: *ep*). Vas deferens inserted subterminally in epiphallus (Figs 36, 37: *vd*). Internal penial surface lacking clear sub-chambers (Fig. 36: *pe*); except for 2–4 longitudinal narrow, separated, slightly equidistant folds (Fig. 37: *pe*). Penis sheath absent.

Central nervous system (Fig. 38). Nerve ring located just posterior to buccal mass (Fig. 27: *ce*, *pp*). Cerebral ganglia located dorsally, pedal ganglia located more anteriorly, about in middle level of buccal mass (Fig. 27). Pair of cerebral ganglia (*ce*) located close
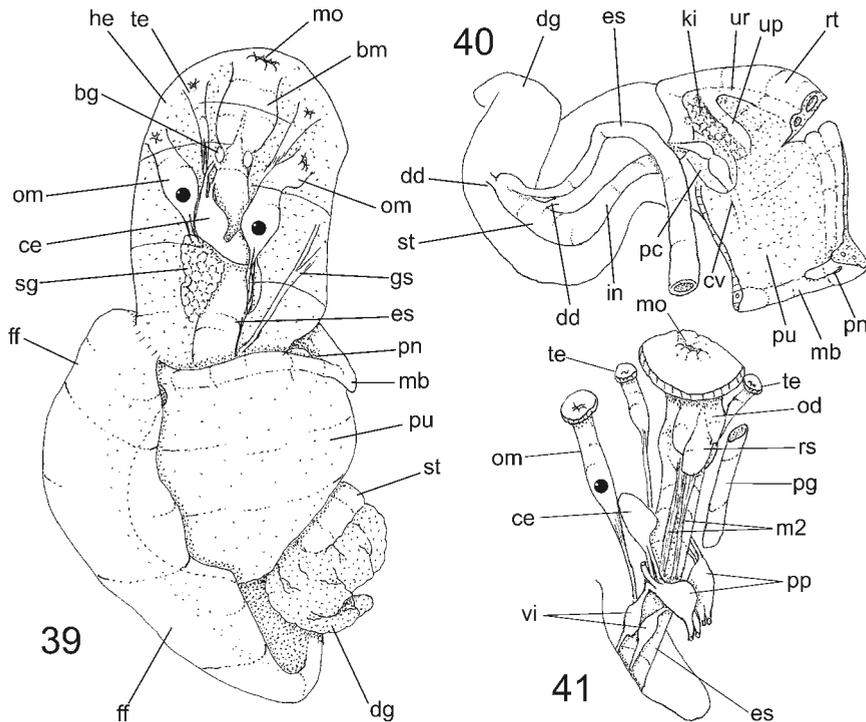
Figs 39–41. *Lavajatus moroi* anatomy of intrauterine specimens. **39.** Whole dorsal view, shell removed, some haemocoel structures seen by transparency; **40.** pallial cavity and visceral mass, mostly ventral view, topology of midgut seen as in situ; **41.** structures of haemocoel, ventral-slightly right view, integument mostly removed. Scale = 1 mm.

with each other; cerebral commissure with ~$\frac{1}{2}$ each ganglion width and ~$\frac{1}{4}$ its length; each ganglion about as wide as adjacent esophageal section; several wide nerves originating in cerebral lateral region. Cerebral node (also called optical ganglion or gland) located in antero-lateral quadrant, with ~$\frac{1}{5}$ each ganglion's size (*gl*). Two pairs of parallel connectives (*cn*) longer connective (~ twice cerebral ganglion length) between cerebral ganglia and pedal ganglia; shorter (ventral) connective (~$\frac{1}{2}$ previous connective length) between cerebral and pleural ganglia. Pair of pleural ganglia with ~$\frac{1}{5}$ cerebral ganglia size, elliptical (~ twice longer than wide), located closer to pedal ganglia, connected to it by short connective (~$\frac{1}{2}$ pleural ganglion length). Pair of pedal ganglia (*pp*) close from each other, pedal commissure almost imperceptible, slightly smaller sized than cerebral ganglia. At least three pairs of pedal nerves originating from anterior side of these ganglia. Pair of statocysts located in anterior-ventral region of pedal ganglia, with ~$\frac{1}{10}$ each ganglion size. Visceral or subesophageal ganglion very large (*vi*), located ventrally to pedal ganglia, size about as large as both pedal ganglia; right short connective with right pleural ganglion; two short left connectives

(slightly placed more posterior) with left pleural and left pedal ganglia.

Ontogeny (Figs 8, 9, 39–41). Studies on young specimens found inside uterus permitted comparison with adult specimens above described. The following differences or remarkable features are found:

Head-Foot. Despite in having some few (~20 %) of the intrauterine specimens completely retracted inside the shell, most of them are preserved expanded. The head are normally very swollen. Its transparent walls permit easy visualization of the internal structures (Figs 7–8), including retracted ommatophore (Fig. 39: *om*) and tentacles (*te*). The retractor muscles of the ommatophores and tentacles are interestingly surrounding the adjacent portions of foregut towards posterior, from dorsal to ventral (Fig. 39), inserting in columellar muscle (this same feature is found in the adults, but with a slightly more complex way through foregut and local portion of genital structures). The foot always has a posterior, wide flap, sometimes called pedal vesicle (e. g., Dutra 1988). This posterior flap can be preserved turned anteriorly (Fig. 8), but normally it is preserved turned posteriorly (Figs 7, 39: *ff*), covering ventral surface of the shell. The pedal

gland is proportionally much larger (Fig. 41: *pg*), emerging from the haemocoel floor, running along middle-posterior levels of haemocoel ventral region.

Pallial cavity. The usual structures are relatively similar to the adult model, except in being very shorter, smaller than 1-whorl long (Fig. 40: *pu*), with structures more simplified (see, e. g., the ureter – Fig. 40: *up*, *ur*; relative to the Fig. 21). The mantel border (*mb*) is also similar to the adult structure.

Visceral mass. It is only 2-whorl long, but, despite in being much shorter (Figs 39, 40), it has a similar organization as adult structures, with the stomach (*st*) located in inferior/columellar surface, and a white digestive gland occupying the rest (*dg*).

Digestive system. The digestive tubes are considerably shorter (~3-whorl long) and wider; internally the digestive tubes are simpler, lacking folds or divisions. The radula is relatively similar to the above described for the adult (Figs 17–20), except in having fewer teeth per row (Fig. 17), 8–10 pairs of teeth per row, lacking rachidian. Lateral teeth with ~5 pairs (Fig. 17, 19), also possessing pair of intercalated cusps; each cusp slightly shorter and thicker than those of adults. Marginal teeth ~4–5 pairs also bicuspid; cusps slightly aligned (except for more central teeth) (Figs 18, 20). The stomach (*st*) is also shorter, but already possessing both ducts to digestive gland (Fig. 40: *dd*), and no clear division with intestinal origin (*in*). The intestine is considerably shorter and simple, being simply sigmoid in region posterior to pallial cavity (Fig. 30: *in*).

Genital system. It is naturally reduced, being only hardly visible anteriorly, crossing the right region of swollen head (Figs 7, 8, 39: *gs*).

Central nervous system. It is the structure that has higher modification if compared to the adult specimens. In the young specimens (Figs 39, 41), the cerebral (*ce*) and pedal (*pp*) ganglia are similar sized and shaped compared to the adult (Fig. 38), despite in being proportionally more closely located from each other, and all them located more posteriorly, at middle esophageal level, far removed from the buccal mass (Fig. 41). The adult pleural ganglion (Fig. 38: *gp*) is not distinguishable in the young specimens (Fig. 41), which possibly will develop later in the ventral connective between cerebral and pedal ganglia. The visceral/subesophageal ganglion is single, large, and placed ventral to the pair of pedal ganglia in adult (Fig. 38: *vi*), while it is a pair of small ganglia in young specimens (Fig. 41: *vi*), in such commissure is very short, and they are located at some distance from the nerve ring, dislocate to the right.

The long pair of buccal mass retractors pass through the nerve ring in adult (Fig. 27: *m2*), but this is clearer in young specimens (Fig. 41: *m2*), evidenced by the longer distance between the buccal mass and the nerve ring.

Habitat. Found inside caves. Considering the shell fragility and the absence of pigmentation, it is possible the species has troglobian habits. The single discrepant character for a whole troglobian adaptation is the clear presence of eyes, present since the intrauterine specimens.

Distribution. Known from the type locality only.

Measurements (length × width in mm). Holotype: 34.7 by 5.2; paratypes MZSP 131066#1: 30.8 by 4.4; #2: 23.0 by 4.2.

Etymology. The specific epithet is in honor to the judge Sérgio Fernando Moro, professor of criminal law in Federal University of Paraná, who is leading Lava-Jato Operation referred above. This is a demure acknowledge of his effort in remodeling Brazil into a better country.

Discussion

The very elongate, multispiral shell possessing almost straight whorls profile, and absence of sculpture is the main set of shell attributes that leaded the present description of a new genus. Normally the subulinines have a well-marked suture, and whorls with rounded profile (Schileyko 1999). *Lavajatus* has, on the other hand, a resemblance with *Rhodea* H. & A. Adams, 1855 (Grego et al. 2007), which also has a straighter whorls profile; however, *Lavajatus* has a more pointed apex and a more uniform growth (*Rhodea* has a blunter apex and wider growth in the first teleoconch whorls than in middle and inferior whorls), and, as main difference, *Lavajatus* lacks the inferior carina of each whorl, which appear in first teleoconch whorls and becomes much pronounced in last whorls in *Rhodea*; some species, e. g., *Rhodea cousini* Jousseaume, 1900, form an outstanding peripheral carina in whorls preceding aperture, which naturally produces a triangular aperture (Grego et al. 2007: fig. 19). No other South American subuline genus has any resemblance with *Lavajatus*. In other mainland, the new genus weakly resembles *Glessula* Martens, 1860, *Prosopeas* Mousson, 1857 (both from Asia), *Homorus* Albers, 1850 (Africa), *Leptopeas* Baker, 1927 (Central America), but differs by the multispiral shell shape, larger size, flattened last whorl, and straight profile. From South American *Neobeliscus* Pilsbry, 1896 and *Obeliscus* Beck, 1837, *Lavajatus* further differ in being smaller-sized, straight profile,

flattened last whorl, multispiral shape, and, mainly, by much sharper-pointed apex. Related to the multispiral shape, with each whorl relatively narrow, it is only compared in South American to *Beckianum* Baker, 1961, from which *Lavajatus* differs in being much larger, straight profile and with uniform growth (*Beckianum* has wider growth near apex and somewhat cylindrical in the rest).

Baker (1927, 1945) reported the foot with grooves as characteristic of subulinines, however, this feature was not found in *L. moroi*. Although only retracted fixed species have been examined, which can preclude this analysis. On the other hand, the high degree of retraction of *L. moroi* is decidedly remarkable. In the Figures 1, 4 and 5, yellow bars indicate the empty portions of some examined shells, an easy measure as the shell is translucent. When retracted, *L. moroi* keeps empty ⅓ (Fig. 1) to half (Fig. 3) of inferior shell region. Autotomy of the shell apex is also found in ~30 % of the specimens (Fig. 5). On the other hand, it is not possible to infer if the examined specimens were in any kind of aestivation or passing through phase of scarcity, which supposedly can cause higher retraction. However, nothing in the anatomy indicated that.

The pallial cavity having weakly visible vases appears to be common to most subulinines (Marcus & Marcus 1968), and has been confirmed in *L. moroi*. Normally higher vascularized lungs are seen in larger-sized snails, in such perfusion of gases may be more complicated, while small snails usually have an easier perfusion even though the integument, and the lung can possess a lower richness of vases. *L. moroi* can be ranked as large for a subulinine, but retains the scarcity of lung vessels (Fig. 23).

Lavajatus moroi has maintained the subulinine character of having an elongated kidney, longer than the pericardium (Baker 1927), as happens in families of, e. g., Bulimuloidea. This possibly implicates in an evolutionary trend. On the other hand, a narrow anterior projection, compressed between primary ureter and pericardium (Fig. 29) appears to be exclusive of *L. moroi*.

A muscular epiphallus, with the vas deferens inserted subterminally, have been found in other subulinines (Baker 1927, Marcus & Marcus 1968); it is also found in *L. moroi* (Fig. 37: ep) and may be another family's feature, despite in being a plesiomorphy. At least in *Paropeas achatinaceum* (Pfeiffer, 1846), the muscular epiphallus looks still more complex, having some internal subdivisions (Naggs 1994: figs 17, 18).

Another feature that appear to be characteristic of subulinines is the attachment of the penis retractor muscle directly into the columellar muscle (Fig. 36: *pm*), at least in the species in which this character had been investigated (Naggs 1994: fig. 19). The more

common state of pulmonates (Simone 2011) is the penis muscle originated in the middle or posterior region of diaphragm, in the muscular floor of the pallial cavity.

The presence of multiple seminal receptacles of *L. moroi* (Fig. 34: sr) appears to be unique. Normally the structure is a single, small, balloon-like diverticulum at the base of the hermaphrodite duct in the examined subulinines (Wille 1915, Baker 1927, Hausdorf et al. 2012), as well as in most stylommatophorans. The gonad of all subulinines appears to be small, as some minute, separated, bulk of acini (Fig. 33: go) (Baker 1927, Marcus & Marcus 1968, Naggs 1994).

The incubation of ova, embryos, and even young specimens inside uterus appears to be a common character in Achatinoidea (Baker 1927, 1945). Some subulinine species bring only ova (e. g., *Leptinaria lamellata* (Potiez & Michaud, 1838) – Baker 1927: fig. 20-1, Carvalho et al. 2009; *Paropeas achatinaceum* – Naggs 1994: fig. 13), while others bring ova, embryos to young specimens, as *L. moroi* (e. g., *Neosubulina scopulorum* Baker, 1924, 1927: fig. 22-11; *Leptinaria unilamellata* (d'Orbigny, 1835) – Dutra 1988).

Comparing the anatomical attributes of *L. moroi* with another supposed subulinine, *Synapterpes hanleyi* (Pfeiffer, 1846) (Salgado & Coelho 1999) little in common appear in these similar-sized species. *S. hanleyi* has a more globose shell, the protoconch has only a single whorl, the lung has high-developed vessels, the jaw is well-developed, the gonad is large, the penis is complex, with some inner subdivisions, and, mainly, it has no indication of brood embryos or young specimens in uterus. These characters look more closely related to Bulimulidae rather than Subulininae. Based on these features, it is rather possible that *S. hanleyi*, as described by Salgado & Coelho (1999), actually belongs to Bulimulidae.

The anatomical study of the intrauterine young specimens of *L. moroi* demonstrated some radical changes in some structures, most of them explored in the description above (Ontogeny section). Possibly, these changes can be extrapolated to other subulinines. Some of the principal ontogenetic modifications are the large elongation of the haemocoelic, pallial and visceral structures, promoted by the intense shell coiling. All these structures are 1-whorl long in young specimens, but are 5–7-whorl long in adult ones. This qualified large elongation keeps relatively empty some portions of these body regions, such as, e. g., the posterior half of the haemocoel (Fig. 24). Another distinction is the absence of intestinal coiling in young specimens (Fig. 40), which are present in adult ones (Fig. 25: *in*). In the central nervous system, the visceral/subesophageal ganglion is a pair in the young specimens (Fig. 41: *vi*), weakly dislocated to

right, located posteriorly from the nerve ring. These both ganglia fuse with each other and dislocate anteriorly during the development, being located at level of nerve ring in adult specimens (Fig. 38: *vi*), in a single, relatively large ganglion. The double origin of this adult ganglion is intriguing, and keep some doubt if it actually is a visceral ganglion strangely dislocated anteriorly, or a subesophageal ganglion. In both cases, these ganglia are supposed of single origin. Another explanation could be an approaching of both ganglia, or another else (e.g., parietal ganglion) in the young, with further fusion in the adult. Another interesting youthful feature is the large size of the pedal gland (Fig. 41: *pg*), which is not easily visible in the adult. It is intrigant what such gland is used for in intrauterine specimens, despite their modified large foot, possessing a wide posterior flap (Fig. 39: *ff*).

Young specimens inside uterus is inquiring in respect to how they can feed and breathe. Ova and embryos can extract their energy direct from the yolk, but possibly intrauterine young specimens need further amount of energy for growing at least 2 more whorls in the case of *L. moroi* and other subulinines. The complete and developed digestive system (including the radula – Figs 17–20) of the young intrauterine specimens (Figs 39–41) indicates that they can eat inside uterus, an assertion so far speculative. The tip portion of the spermoviduct of all examined specimens has thick glandular walls and always lacks specimens inside (Figs 33, 34: *eo*). Possibly this region of the spermoviduct produce some kind of nutritive mucus, in such the young specimens can ingest. No other apparent kind of food source was found in uterus, such as nurse-eggs or extra-yolk, which the young specimens can use for growing up. The posterior flap of the foot has been inferred as a possible alimentary adaptation (e.g., Dutra 1988, as pedal vesicle). However, the posterior pedal flap looks more useful for breathing than for eating. It is intuitive to infer that the respiratory activity of the intrauterine young specimens may be via diffusion, in such the gases flow from pallial (pulmonary) cavity, through diaphragm-integument, up to uterus itself. The young specimen can use this mechanism for breathing, and the surface enlargement provided by the pedal posterior flap and the swollen head look convenient (Fig. 39), as the lung itself appear to be small (Fig. 40: *pu*). Some subulinines have their intrauterine offspring enclosed in a thin, individual membrane (Tompa 1979, Carvalho et al. 2009), which possibly indicates a non-alimentary intrauterine phase, a feature not found in *L. moroi*.

References

Almeida, M. N. & Bessa, E. C. A. 2001. Estudo do crescimento e da reprodução de *Leptinaria unilamellata* (d'Orbigny) (Mollusca, Subulinidae) em laboratório. Revista Brasileira de Zoologia 18 (4): 1107–1113.

Baker, H. B. 1927. The Mollusca collected by the University of Michigan-Williamson Expedition in Venezuela. Occasional Papers of the Museum of Zoology 182: 1–36, pls 20–26.

– – 1945. Some American Achatinidae. Nautilus 58: 84–92.

Budha, P. B., Naggs, F. & Backeljau, T. 2017. Conchological differentiation and genital anatomy of Nepalese Glessulinae (Gastropoda, Stylommatophora, Subulinidae), with descriptions of six new species. Zookeys 675: 129–156. doi:10.3897/zookeys.675.13252

Carvalho, C. M., Silva, J. P., Mendonça, C. L. F., Bessa, E. C. A. & D'ávila, S. 2009. Life history of *Leptinaria unilamellata* (d'Orbigny, 1835) (Mollusca, Pulmonata, Subulinidae). Invertebrate Reproduction and Development 53 (4): 211–222.

Dutra, A. V. C. 1988. Aspectos da ecologia e da reprodução de *Leptinaria unilamellata* (Orbigny, 1835) (Gastropoda, Subulinidae). Revista Brasileira de Zoologia 5 (4): 581–591.

Fontanilla, I. K. C., Naggs, F. & Wade, C. M. 2017. Molecular phylogeny of the Achatinoidea (Mollusca: Gastropoda). Molecular Phylogenetics and Evolution 114. doi:10.1016/j.ympev.2017.06.014

Grego, J., Šteffek, J. & Infante, A. P. 2007. Review of the genus *Rhodea* (Gastropoda, Pulmonata, Subulinidae) with description of two new species from Colombia. Basteria 71: 13–28.

Hausdorf, B., Kroll, O. & López-Victoria, M. 2012. The land snails of Malpelo Island, Colombia. Journal of Molluscan Studies 78: 157–165.

Marcus, Ev. & Marcus, Er. 1968. Über einige Subulinidae (Pulmonata von São Paulo). Beiträge zur Neotropischen Fauna 5: 186–208. doi:10.1080/01650526809360407

Mead, A. R. 1950. Comparative genital anatomy of some African Achatinidae (Pulmonata). Bulletin of the Museum of Comparative Zoology 105: 219–291, pls 1–9.

Naggs, F. 1994. The reproductive anatomy of *Paropeas achatinaceum* and a new concept of *Paropeas* (Pulmonata: Achatinoidea: Subulinidae). Journal of Molluscan Studies 60 (2): 175–191.

Pilsbry, H. A. 1906. Achatinidae: Stenogyridae and Coeliaxinae. Manual of Conchology, Ser. 2, 18: 1–357.

Salgado, N. C. & Coelho, A. C. S. 1999. Recharacterization of *Synapterpes* (*S.*) *hanleyi* (Pfeiffer) (Mollusca, Gastropoda, Stylommatophora, Subulinidae). Revista Brasileira de Zoologia 19 (3): 621–628.

Schileyko, A. A. 1999. Treatise on recent terrestrial pulmonate molluscs 4. Ruthenica Suppl. 2: 435–564.

Simone, L. R. L. 2006. Land and freshwater molluscs of Brazil. 390 pp., São Paulo (FAPESP, EGB).

– – 2011. Phylogeny of the Caenogastropoda (Mollusca), based on comparative morphology. Arquivos de Zoologia 42 (4): 161–323.

– – 2012a. Taxonomical study on a sample from Santa Maria da Vitória, Bahia, Brazil, with description of a new genus and four new species (Mollusca: Orthalicidae and Megalobulimidae). Papéis Avulsos de Zoologia 52 (36): 431–439.

– – 2012b. A new genus and species of cavernicolous Pomatiopsidae (Mollusca, Caenogastropoda) in Bahia, Brazil. Papéis Avulsos de Zoologia 52 (40): 515–524.

– – 2013. *Habeas*, a new genus of Diplommatinidae from central Bahia, Brazil (Caenogastropoda), with description of three new species. Journal of Conchology 41 (4): 519–525.

Tompa, A. S. 1979. Oviparity, egg retention and ovoviviparity in pulmonates. Journal of Molluscan Studies 45: 155–160.

Wille, J. 1915. Untersuchungen über den anatomischen Bau der Lungenschnecke *Stenogyra decollata* L. Jenaische Zeitschrift für Naturwissenschaft 53: 717–803.